

Photoluminescence Broadening Induced by Internal Electric Field Variations in Polar InGaN/GaN Quantum Wells

Nguyen Thi Phuong Loan^{1*}, Phan Xuan Le², Phan Thi Minh Man³

¹Faculty of Fundamental 2, Posts and Telecommunications Institute of Technology, Ho Chi Minh City, 70000, Vietnam

²Faculty of Electrical Engineering Technology, Industrial University of Ho Chi Minh City, Ho Chi Minh City, 70000, Vietnam

³Faculty of Electrical and Electronics Engineering, Ton Duc Thang University, Ho Chi Minh City, 70000, Vietnam

*Corresponding author: ntploan@ptithcm.edu.vn

Abstract

This study investigates the influence of internal electric field modulation on photoluminescence (PL) broadening in polar InGaN/GaN quantum wells (QWs). By applying an external bias, the internal electric field is effectively controlled, allowing systematic evaluation of its role in spectral broadening. Photoluminescence and electro-reflectance measurements reveal that reducing the internal electric field leads to a noticeable narrowing of the PL linewidth. A theoretical model is developed to describe the relationship between electric field fluctuations and emission energy variation. The results indicate that stronger internal electric fields enhance the sensitivity of emission energy to local potential fluctuations, thereby increasing PL broadening. Additionally, a reduction in the Huang-Rhys factor is observed under decreased electric field conditions, suggesting weakened exciton-phonon coupling. These findings provide direct experimental evidence of the role of internal electric fields in PL broadening and offer a pathway for spectral control in III-nitride optoelectronic devices.

Keywords

InGaN/GaN, Quantum Wells, Photoluminescence, Electric Field, QCSE, Spectral Broadening

Received: 24 February 2026, Accepted: 11 May 2026

<https://doi.org/10.26554/ijmr.20264388>

1. INTRODUCTION

InGaN/GaN quantum wells (QWs) have emerged as a cornerstone in modern optoelectronic devices, particularly in light-emitting diodes (LEDs) and laser diodes, due to their tunable emission wavelength and high quantum efficiency. The emission properties of these structures can be engineered through indium composition, well thickness, and strain distribution, enabling applications across a broad spectral range (Lin et al., 2021; Francis et al., 2020). A notable feature of InGaN QWs is strong carrier localization caused by compositional fluctuations, which enhances radiative recombination efficiency even in the presence of defects (Yoshimura et al., 2019; Lin et al., 2021).

In polar InGaN/GaN quantum wells, internal electric fields arising from spontaneous and piezoelectric polarization significantly influence optical properties through the quantum confined Stark effect (QCSE). This effect induces a redshift in emission energy and reduces electron-hole wavefunction overlap, thereby modifying recombination dynamics. In addition to QCSE, structural inhomogeneities such as indium clustering, thickness variations, and strain fluctuations contribute to photoluminescence (PL) broadening (Chlipala et al., 2020; Zhang et al., 2019).

Although numerous studies have investigated PL broaden-

ing in InGaN QWs, the direct contribution of internal electric field variations remains insufficiently quantified. In most previous works, electric field effects are indirectly modified through structural parameters, making it difficult to isolate their intrinsic role. This limitation creates ambiguity in distinguishing between structural disorder effects and electric-field-induced broadening mechanisms (Gao et al., 2021; Hassan et al., 2020).

To address this gap, this study proposes a direct experimental approach by modulating the internal electric field using an external bias. This method allows for decoupling electric field effects from structural inhomogeneities, providing a clearer understanding of their role in PL broadening.

The novelty of this work focuses on applying an external bias to directly influence inner fields of electricity, enabling a more precise investigation of their intrinsic effects. Furthermore, this study provides experimental validation of electric-field-induced spectral broadening, which has not been clearly isolated in previous studies. In addition, a theoretical framework is developed to quantitatively describe the relationship between electric field fluctuations and emission linewidth, offering deeper insight into the underlying physical mechanisms. This paper is organized as follows: the experimental methodology is described in Section 2, followed by detailed results and discussion in Section 3, where

both experimental observations and theoretical analysis are presented. Finally, conclusions and implications for optoelectronic device optimization are summarized.

2. EXPERIMENTAL SECTION

2.1 Materials and Structure

The InGaN/GaN quantum well structure was synthesized utilizing metal-organic chemical vapor deposition (MOCVD). The layout consists of a Si-doped GaN buffer layer deposited on a c-plane GaN substrate, followed by multiple InGaN quantum wells divided by GaN barriers. A Mg-doped AlGaIn electron blocking sheet and a Mg-doped GaN sheet were subsequently deposited.

2.2 Instrumentation

Photoluminescence (PL) measurements were performed utilizing a Ti:sapphire laser with a wavelength of 800 nm and a repetition rate of 80 MHz. The emitted signal was dispersed using a monochromator and detected using a nitrogen-cooled CCD system. Electro-reflectance measurements were performed using a lock-in detection system with combined AC and DC bias.

2.3 Experimental Procedure

An external bias ranging from 0 to -5 V was applied to modulate the inner field of electricity in the quantum wells. All measurements were conducted at room temperature. The PL spectra were analyzed using Gaussian fitting to extract linewidth and peak position. Electro-reflectance spectroscopy was used to verify energy transitions.

3. RESULTS AND DISCUSSION

The photoluminescence (PL) spectra of the quantum wells were measured under different applied bias conditions to investigate the effect of internal electric field modulation. At zero bias, the PL spectrum exhibits an asymmetric profile with a noticeable low-energy tail, which can be attributed to phonon replicas. The full width at half maximum (FWHM) is relatively large due to contributions from both ground-state emission and phonon-assisted transitions. As the reverse bias increases, the inner field of electricity within the quantum wells is reduced. Consequently, a clear blue-shift of the PL peak is seen, followed by a notable narrowing of the emitting linewidth. In addition, the spectral shape becomes more symmetric, and the contribution of phonon replicas is gradually suppressed.

This behavior can be explained by the enhanced overlap between electron and hole wavefunctions under reduced electric field conditions, which weakens exciton-phonon coupling. The decrease in the Huang-Rhys factor further supports this interpretation. Gaussian fitting of the PL spectra reveals that the linewidth reduction is primarily associated with the ground-state transition.

To further interpret these results, it is important to compare them with previous studies on QCSE-induced spectral broadening. Similar trends of linewidth reduction under decreasing electric field have been reported (Zhang et al., 2020; Gao et al., 2021),

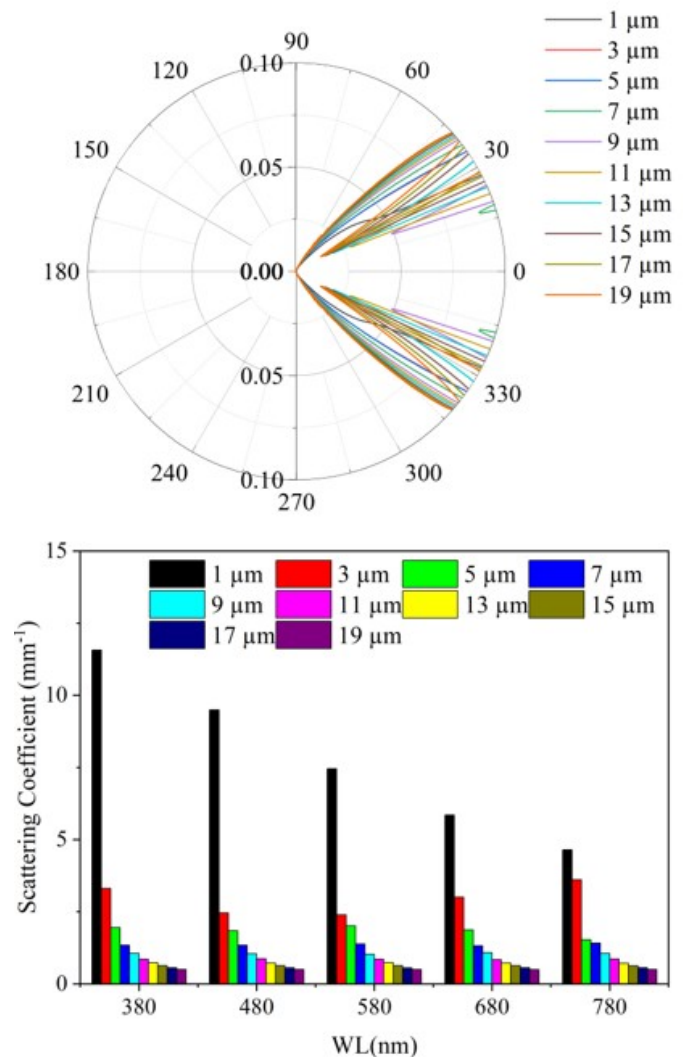


Figure 1. Relationship Between Scattering Coefficient and Wavelengths

where reduced field strength enhances electron-hole overlap and suppresses localization effects. However, unlike earlier works where structural parameters were varied simultaneously, the present study isolates the electric field contribution, providing clearer evidence of its intrinsic role. The observed reduction in linewidth can be attributed to decreased sensitivity of transition energy to local electric field fluctuations. According to Equation (2), the broadening is proportional to the derivative dE/dF , which becomes smaller as the internal electric field decreases. This explains the improved spectral symmetry and reduced phonon replica intensity.

Despite these findings, several limitations should be noted. The study assumes uniform field modulation across the quantum well, whereas local variations may still exist. Additionally, temperature-dependent effects were not explored and may influence exciton-phonon interactions.

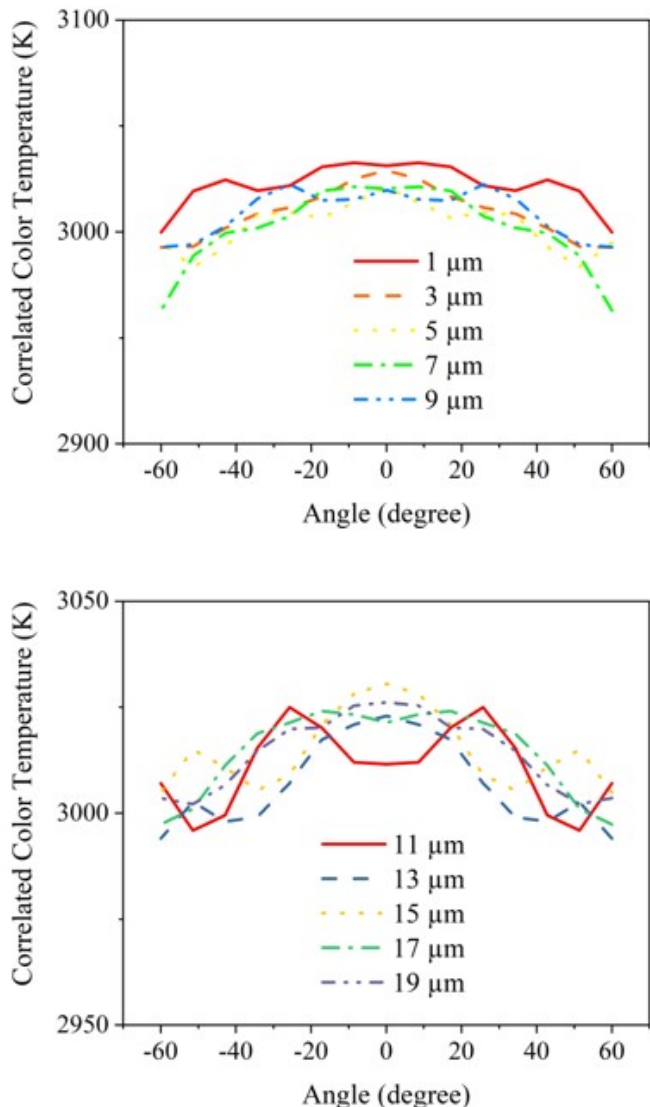


Figure 2. CCT Alteration Based on Particle Size

These results have important implications for LED design. By controlling internal electric fields through device engineering or external bias, it is possible to achieve narrower emission spectra and improved color purity. This is particularly relevant for micro-LED and display technologies where spectral precision is critical. To describe the effect of the inner field of electricity on the emission energy in quantum wells, the quantum confined Stark effect (QCSE) can be expressed as in Equation (1):

$$E = E_0 - pF + \beta F^2 \tag{1}$$

where E is the transition energy under a field of electricity, E_0 is the transition energy in the absence of an electric field, F is the inner field of electricity, p represents the built-in dipole moment, and β is the polarizability constant. This equation shows that the emission energy strongly depends on the magnitude of the

internal electric field.

The contribution of electric field fluctuations to photoluminescence broadening can be approximated by Equation (2):

$$\Delta E \propto \frac{dE}{dF} \cdot \Delta F \tag{2}$$

where ΔE is the energy broadening, ΔF represents fluctuations in the local electric field, and dE/dF describes the sensitivity of the emission energy to electric field variations. This relationship indicates that stronger internal electric fields amplify the effect of local field fluctuations, leading to increased spectral broadening. Therefore, reducing the internal electric field using an external bias is expected to decrease the emission energy variation and consequently narrow the photoluminescence spectrum.

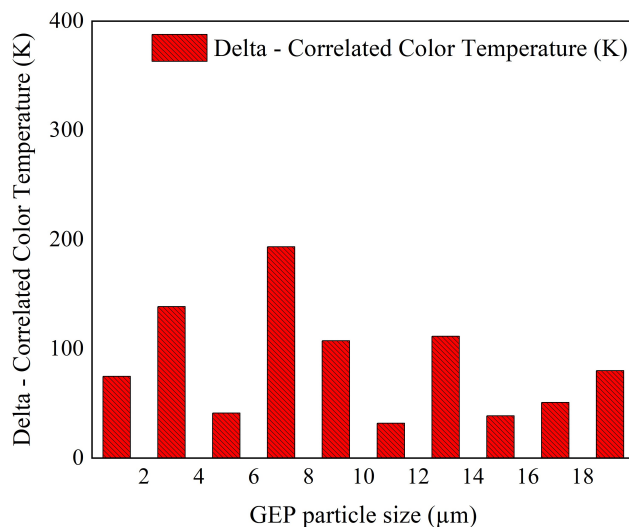


Figure 3. Variation in Hue Aberration Under SiO₂ Particle Size

Figure 1 shows the dependence of the scattering coefficient on angle, wavelength, and particle size. The polar plot indicates that scattering is mainly concentrated in the forward direction (around 0°) and decreases at larger angles, demonstrating anisotropic behavior. The bar chart reveals that the scattering coefficient is higher at shorter wavelengths and decreases as the wavelength increases. Additionally, larger particle sizes result in stronger scattering across all wavelengths due to increased scattering cross-section. Overall, both wavelength and particle size significantly influence the scattering behavior. Particle size plays a crucial role in determining CCT characteristics, as illustrated in Figure 2. At a particle size of 11 wt.%, the CCT exhibits the largest variation. The minimum CCT value occurs at 7 wt.%, whereas the maximum is observed at 15 wt.%.

Hue deviation varies with particle size, as presented in Figure 3. A pronounced increase is observed at 7 wt.%, while the lowest values are recorded at 5, 11, and 15 wt.%. For the lumen output shown in Figure 4, a consistent decrease is noted as the particle size increases from 1 to 5 μm. Beyond this range, the

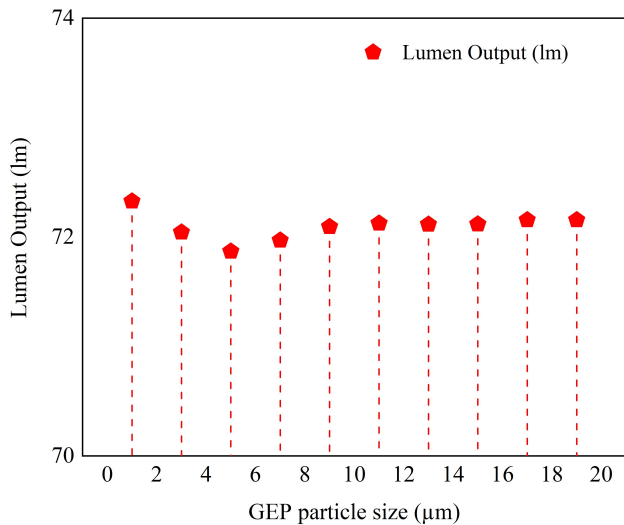


Figure 4. LED Lumen Generated Based on SiO₂ Particle Size

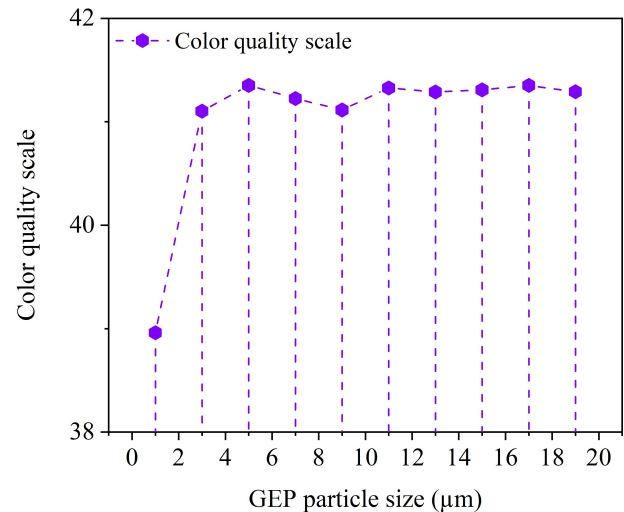


Figure 6. CQS Values with Various SiO₂ Proportions

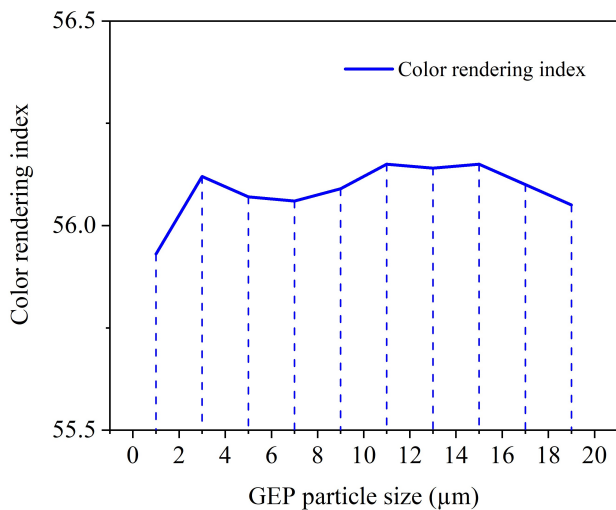


Figure 5. CRI Values with Various SiO₂ Proportions

lumen remains relatively stable with only minor fluctuations. These trends can be attributed to variations in color distribution and reduced blue-light intensity caused by enhanced backward scattering and repeated absorption.

As particle size increases, the phosphor layer tends to thicken, which lowers the overall spectral energy. Consequently, the conversion between blue light and longer wavelengths (yellow or red-orange) becomes more pronounced. This suggests that, at very large particle sizes, a portion of the transmitted light undergoes back-reflection, leading to a reduction in luminous intensity and an increase in CCT (Chen et al., 2021; Chung et al., 2019; Wang and Zhu, 2018).

As seen in Figures 5 and 6, particle size has a major impact on the brightness and hue rendition of white LEDs. Color rendition measurements using CRI and CQS revealed a slight increase with

particle sizes of 1-3 μm, with CRI values rising from ~55.8 to ~56.2 and CQS values rising from ~39 to ~41. They remained stable at the same period, with particle sizes ranging from 4 to 19 μm with the CRI values of about 56.2 and CQS values of about 41.5. The colors blue, green, and yellow-orange may have lower CRI and CQS because of their unpredictable nature. Larger particle sizes result in better dispersion and irregular light emission those trends toward the yellow-orange spectrum. As we assess the results, we will adjust the CRI and CQS of this phosphor and take other factors like particle size into account.

4. CONCLUSIONS

In conclusion, this study demonstrates that internal electric field variations play a crucial role in photoluminescence broadening in polar InGaN/GaN quantum wells. By applying an external bias, we directly modulated the electric field and observed a significant reduction in PL linewidth. Both experimental results and theoretical analysis confirm that stronger electric fields enhance the sensitivity of emission energy to local fluctuations, leading to spectral broadening. Additionally, reduced exciton-phonon coupling was observed under weaker electric field conditions. These findings provide a deeper understanding of the mechanisms governing PL broadening and offer practical strategies for improving spectral performance in III-nitride optoelectronic devices.

5. ACKNOWLEDGEMENT

The authors wish to express their gratitude to the Posts and Telecommunications Institute of Technology, Vietnam, for financial support for this research.

REFERENCES

Chen, D., Z. Wang, F. Hu, C. Shen, N. Chi, W. Liu, and H. Lu (2021). Improved Electro-Optical and Photoelectric Performance of

- GaN-Based Micro-LEDs with an Atomic Layer Deposited AlN Passivation Layer. *Optics Express*, **29**(22); 36559
- Chlipala, M., H. Turski, M. Siekacz, K. Pieniak, K. Nowakowski-Szkudlarek, T. Suski, and C. Skierbiszewski (2020). Nitride Light-Emitting Diodes for Cryogenic Temperatures. *Optics Express*, **28**(20); 30299
- Chung, K., J. Sui, T. Sarwar, and P. Ku (2019). Feasibility Study of Nanopillar LED Array for Color-Tunable Lighting and Beyond. *Optics Express*, **27**(26); 38229
- Francis, K. J., Y. E. Boink, M. Dantuma, M. K. A. Singh, S. Manohar, and W. Steenbergen (2020). Tomographic Imaging with an Ultrasound and LED-Based Photoacoustic System. *Biomedical Optics Express*, **11**(4); 2152
- Gao, X., Y. Xu, J. Huang, Z. Hu, W. Zhu, X. Yi, and L. Wang (2021). Circularly Polarized Light Emission from a GaN Micro-LED Integrated with Functional Metasurfaces for 3D Display. *Optics Letters*, **46**(11); 2666
- Hassan, A., S. Khan, K. Rasul, and A. Hussain (2020). Lensless On-Chip LED Array Microscope Using Amplitude and Phase Masks. *Journal of the Optical Society of America B*, **37**(12); 3652
- Lin, S., M. Tseng, K. Peng, S. Lai, M. Shen, R. Horng, and Z. Chen (2021). Enhanced External Quantum Efficiencies of AlGaIn-Based Deep-UV LEDs Using Reflective Passivation Layer. *Optics Express*, **29**(23); 37835
- Wang, W. and P. Zhu (2018). Red Photoluminescent Eu³⁺-Doped Y₂O₃ Nanospheres for LED-Phosphor Applications: Synthesis and Characterization. *Optics Express*, **26**(26); 34820
- Yoshimura, R., D. Choi, M. Fujimoto, A. Uji, F. Hiwatashi, and K. Ohbayashi (2019). Dynamic Optical Coherence Tomography Imaging of the Lacrimal Passage with an Extrinsic Contrast Agent. *Biomedical Optics Express*, **10**(3); 1482
- Zhang, A., Y. Chen, Z. Wu, S. Zhang, Z. Zhu, L. He, and S. Yu (2019). Enhanced Amplified Spontaneous Emission from Conjugated Light-Emitting Polymer Integrated with Silicon Nitride Grating Structures. *OSA Continuum*, **2**(10); 2875
- Zhang, T., X. Zhang, B. Ding, J. Shen, Y. Hu, and H. Gu (2020). Homo-Epitaxial Secondary Growth of ZnO Nanowire Arrays for a UV-Free Warm White Light-Emitting Diode Application. *Applied Optics*, **59**(8); 2498